

**This is the final draft of the contribution published as:**

**Türkowsky, D., Lohmann, P., Mühlenbrink, M., Schubert, T., Adrian, L., Goris, T., Jehmlich, N., von Bergen, M. (2019):**

Thermal proteome profiling allows quantitative assessment of interactions between tetrachloroethene reductive dehalogenase and trichloroethene

*J. Proteomics* **192**, 10 – 17

**The publisher's version is available at:**

<http://dx.doi.org/10.1016/j.jprot.2018.05.018>

1       **Thermal Proteome Profiling Allows Quantitative Assessment of Interactions**  
2       **between Tetrachloroethene Reductive Dehalogenase and Trichloroethene**

3       **Dominique Türkowsky<sup>§,1</sup>, Patrick Lohmann<sup>§,1</sup>, Marie Mühlenbrink<sup>1</sup>, Torsten Schubert<sup>2</sup>,**  
4       **Lorenz Adrian<sup>3,4</sup>, Tobias Goris<sup>2</sup>, Nico Jehmlich<sup>1</sup>, Martin von Bergen<sup>1,5</sup>**

5       <sup>1</sup>Department of Molecular Systems Biology, Helmholtz Centre for Environmental Research –  
6       UFZ, Permoserstraße 15, 04318 Leipzig, Germany

7       <sup>2</sup>Department of Applied and Ecological Microbiology, Institute of Microbiology, Friedrich  
8       Schiller University, 07743 Jena, Germany

9       <sup>3</sup>Department of Isotope Biogeochemistry, Helmholtz Centre for Environmental Research –  
10       UFZ, Permoserstraße 15, 04318 Leipzig, Germany

11       <sup>4</sup>Chair of Geobiotechnology, Technische Universität Berlin, Ackerstraße 76, 13355 Berlin

12       <sup>5</sup>Institute of Biochemistry, Faculty of Life Sciences, University of Leipzig, Brüderstraße 34,  
13       Germany

14       <sup>§</sup>These authors contributed equally to this work

15

16       Correspondence:

17       Prof. Dr. Martin von Bergen

18       E-mail: martin.vonbergen@ufz.de, Tel: +49-341-235-1211

19       Keywords: Proteome interaction; organohalide respiration; TCE; PCE; *Dehalococcoides*  
20       *mccartyi*; quantitative proteomics

21 **Abstract**

22 *Thermal proteome profiling* (TPP) is increasingly applied in eukaryotes to investigate protein-  
23 ligand binding through protein melting curve shifts induced by the presence of a ligand. In  
24 anaerobic bacteria, identification of protein-substrate interactions is a major challenge. We  
25 applied TPP to *Sulfurospirillum multivorans*, which is able to use trichloroethene as electron  
26 acceptor for growth, to investigate the interaction of its tetrachloroethene reductive  
27 dehalogenase PceA with trichloroethene. Several modifications in the protocol (e.g.,  
28 incubation under anaerobic conditions; increasing the temperature range up to 97°C)  
29 extended the protein detection range and allowed the investigation of oxygen-sensitive  
30 proteins. Enzymatic reductive dehalogenation was prevented by omitting the electron donor  
31 during incubations. This enabled detecting the interaction of PceA with trichloroethene and  
32 confirmed that trichloroethene is a substrate of this enzyme. Interestingly, a putative response  
33 regulator showed a similar trend, which is the first biochemical hint for its proposed role in  
34 trichloroethene respiration. We proved that our TPP approach facilitates the identification of  
35 protein-substrate interactions of strictly anaerobic reductive dehalogenases and probably  
36 their regulators. This strategy can be used to identify yet unknown substrate specificities and  
37 possible signal-sensing proteins, and therefore has the potential to elucidate one of the  
38 unresolved fields in research on organohalide-respiring bacteria.

39 **Significance**

40 The assessment of enzyme-substrate or protein-ligand interactions in organohalide-respiring  
41 bacteria is a fundamental challenge. *Thermal proteome profiling* (TPP) allows elucidating  
42 proteome-wide thermal stability changes relying on the sensitivity of modern mass  
43 spectrometry. This gives access to the identification of interactions not detectable with other  
44 methods. In this TPP study, we demonstrate the interactions of a chlorinated substrate with a

45 reductive dehalogenase and potentially with a response regulator, thereby supporting the  
46 response regulator's function in organohalide respiration. The strategy might also be applied  
47 to identify yet unknown substrates of other enzymes in bacteria which are difficult to  
48 investigate or for which only low amounts of biomass are available. The assessment of  
49 enzyme-substrate interactions, which might enable conclusions about enzyme specificities,  
50 represents a new application for TPP.

## 51 **Highlights**

- 52 - *Thermal proteome profiling* (TPP) was modified for analyzing bacterial oxygen-  
53 sensitive enzymes
- 54 - Protein-trichloroethene interactions in organohalide-respiring *Sulfurospirillum*  
55 *multivorans* were identified
- 56 - Interaction of the tetrachloroethene reductive dehalogenase with trichloroethene was  
57 confirmed
- 58 - A first hint for the interaction of a response regulator and a chlorinated ethene was  
59 provided

60

## 61 **Introduction**

62 Many organohalides are hazardous to human health and widely distributed in our  
63 environment [1]. Many of them were prohibited decades ago [2-4] but had been used in  
64 industry and agriculture for a long time and are recalcitrant against biodegradation [5].  
65 Several anaerobic bacteria are capable of reductively dehalogenating organohalides, i.e.,  
66 they use organohalides as a terminal electron acceptor during organohalide respiration [6, 7].  
67 The catalyzing enzymes are the iron-sulfur cluster- and corrinoid-cofactor containing  
68 reductive dehalogenases [8]. There are still many unanswered questions in the research on  
69 organohalide-respiring bacteria, involving the functioning of reductive dehalogenases, their  
70 substrate specificities and regulation [9].

71 *Sulfurospirillum multivorans*—an organohalide-respiring bacterium—produces the  
72 tetrachloroethene reductive dehalogenase PceA, which dechlorinates tetra- and  
73 trichloroethene (TCE) [10] but also brominated phenols [11]. A two-component regulatory  
74 system encoded in close vicinity to *pceA* was predicted to be involved in the transcriptional  
75 regulation of the *pceA* gene expression. However, this has not yet been biochemically proven  
76 [12, 13]. In general, two-component regulatory systems involve a histidine protein kinase  
77 detecting a chemical or physical signal from the environment and transducing this signal into  
78 an intracellular signal cascade by phosphorylating a response regulator. The activated  
79 response regulator usually binds to the DNA and induces or suppresses gene expression  
80 [14].

81 Organohalide-respiring bacteria and their reductive dehalogenases are difficult to investigate  
82 because many are extremely sensitive to oxygen. Additionally, many organohalide-respiring  
83 bacteria grow slowly to low cell densities, and protocols for their genetic modification are not  
84 yet available [15], which hinders, e.g., gene deletion studies. Of special interest for  
85 biochemical investigations and bioremediation is the substrate specificity of reductive

86 dehalogenases. Due to the difficulties in heterologous expression and limited possibilities for  
87 protein purification, approaches such as native polyacrylamide gel electrophoresis coupled to  
88 enzymatic assays and mass spectrometry arose [16] but could not resolve reductive  
89 dehalogenase substrate specificity in all cases [17, 18]. Here, we used *S. multivorans* as a  
90 model organism to investigate substrate specificity of a reductive dehalogenase via *thermal*  
91 *proteome profiling* (TPP), since PceA is a well-studied enzyme and *S. multivorans* one of the  
92 few easier to handle organohalide-respiring bacteria, although genetic modification is  
93 severely hampered also in this bacterium.

94 TPP is a further development of the cellular thermal shift assay on a proteome-wide scale. It  
95 was established by Savitski *et al.* [19] in order to screen the whole proteome in an unbiased  
96 way for potential targets of kinase inhibitors. Both techniques were mostly used for the  
97 analysis of the mechanistic effects of drugs, usually inhibitors of enzymes, or of protein-  
98 protein interactions in mammalian cells [20, 21]. The principle of TPP is that if a protein binds  
99 to its ligand, higher temperatures are needed to denature the protein because part of the heat  
100 energy dissociates the enzyme-ligand-complex. Consequently, the protein's melting  
101 temperature ( $T_m$ ), at which 50% of the protein is denatured and which can be calculated from  
102 its melting curve, is shifted to higher temperatures.

103 In this study, we verified that the TPP method is suitable to analyze protein-TCE interactions  
104 of *S. multivorans*. Due to the oxygen sensitivity of involved enzymes [22], oxygen was  
105 excluded during the cultivation, protein extraction, substrate and temperature incubation. We  
106 quantified the soluble protein fraction by a label-free approach instead of the isotopic labeling  
107 as used by Savitski *et al.* [19], which opens up the TPP method to other applications.

## 108 **Materials and Methods**

### 109 **Anaerobic cultivation and media composition**

110 *Sulfurospirillum multivorans* was cultivated anaerobically with 40 mM pyruvate as an electron  
111 donor and 10 mM PCE (nominal concentration, PCE was added from a 0.5 M stock solution  
112 in hexadecane) as an electron acceptor at 30°C and 120 rpm in a defined mineral medium  
113 [23]. In order to reduce the amount of chlorinated ethenes in the cultures to a minimum but to  
114 obtain cells which still produce PceA, the organism was cultivated for three transfers with  
115 40 mM fumarate as an electron acceptor and 40 mM pyruvate as an electron donor with 10%  
116 inoculum each [24].

### 117 **Cell harvest and lysis**

118 The bacterial cells were harvested after 24 h in the late exponential phase. The culture was  
119 centrifuged under anoxic conditions at 4,800 g for 20 min at 10°C for two times with a  
120 washing step in between using 4 mM L-cysteine in phosphate buffered saline. The cell pellet  
121 was dissolved in 4 mL of an anoxic lysis buffer ensuring preservation of PceA activity  
122 (100 mM Tris-HCl, 4 mM ammonium sulfate, 1x MS-SAFE protease and phosphatase  
123 inhibitor (Sigma-Aldrich, St. Louis, USA) and 2 mM L-cysteine) [10]. Cell lysis was performed  
124 anaerobically by using a FRENCH® press (Thermo Fisher Scientific, Waltham, USA) with a  
125 pressure of 1,000 psi. Cell debris was removed by centrifugation of the cell extract at  
126 20,000 g for 10 min at 10°C. The protein concentration of the supernatant was determined by  
127 using the Bradford assay (Sigma-Aldrich, St. Louis, USA). The quality of the sample  
128 preparation was controlled by photometrical measuring the specific activity of the reductive  
129 dehalogenase PceA in the crude extract on TCE using the synergy™ HT multi detection  
130 microplate reader photometer (BioTek Instruments, Inc., Vermont, USA) under anoxic  
131 conditions [23]. The microplate was sealed with a microseal 'B' film (Bio-Rad, CA, USA) and  
132 measured in an anoxic chamber to avoid oxygen exposure.

### 133 **Preparation of cell extract for thermal proteome profiling**

134 While working in the anoxic chamber, the cell extract was split into two equal sets and  
135 incubated with either 5 mM TCE in ethanol (final concentration) or with the same volume of  
136 ethanol as a control. TCE as the substrate was added to the cell extract under anoxic  
137 conditions by using an eVol xR glass pipette (SGE Analytical Science). Each sample per  
138 condition was further divided into 30 aliquots and transferred into 0.6 mL micro bottles (lab  
139 logistic group GmbH, Meckenheim, Germany) sealed with gas-tight caps. The 60 samples  
140 were sequentially incubated for 3 min with one of ten temperatures between 43°C and 97°C  
141 in a ThermoMixer (Thermo Fisher Scientific, Waltham, USA). The heated samples were  
142 shock-frozen in liquid nitrogen. To separate native from denatured proteins, samples were  
143 ultra-centrifuged at 100,000 g for 20 min at 4°C by using an Optima™ MAX-XP  
144 ultracentrifuge and an ML-130 rotor (Beckman Coulter, Pasadena, USA). The supernatant  
145 containing the soluble protein fraction was used for further analysis.

#### 146 **SDS-PAGE, proteolytic digestion, and peptide extraction**

147 The SDS-PAGE was performed to remove contaminants from the samples, according to the  
148 protocol in Franken *et al.* [25]. 25 µg protein of the lowest temperature point (43°C) and equal  
149 volumes of the other samples were reduced in sample buffer (containing 50 mM dithiothreitol  
150 and 1x lithium dodecyl sulfate, Sigma-Aldrich, St. Louis, USA) for 30 min in a ThermoMixer at  
151 50°C and 700 rpm. Subsequently the samples were alkylated with 100 mM 2-iodoacetamide  
152 for 30 min in the dark at room temperature [25]. After SDS-PAGE and staining with colloidal  
153 Coomassie brilliant blue (Merck, Darmstadt, Germany) overnight, the gel band of each  
154 temperature point containing all proteins was cut out, sliced into smaller gel pieces to  
155 increase accessibility to the protease and destained according to Franken *et al.* [25]. In order  
156 to reduce the number of missed cleavages, proteins in each band were proteolytically  
157 digested using both, 0.6 µg lysyl endopeptidase (Wako Chemicals GmbH, Neuss, Germany)  
158 at 37°C for 4 h and 0.5 µg trypsin (Sigma-Aldrich, St. Louis, USA) at 37°C, overnight [25].

159 Digestion was stopped by adding formic acid (FA) to a final concentration of 0.1%. After  
160 peptide extraction [25, 26], the samples were lyophilized using the freeze-dryer alpha 2-4  
161 LSC (Christ, Osterode, Germany) at 0.1 mbar vacuum and 1,650 mbar pressure (-40°C,  
162 overnight). The extracted peptides were desalted using SOLA $\mu$  plates (Thermo Fischer  
163 Scientific, Waltham, USA). Peptides were dissolved in 0.1% FA and injected into liquid  
164 chromatography-mass spectrometry.

### 165 **LC-MS/MS analysis**

166 Samples were analyzed using a liquid chromatography (HPLC, Ultimate 3000 RSLCnano,  
167 Dionex/Thermo Fisher Scientific, Idstein, Germany) coupled via a TriVersa NanoMate  
168 (Advion, Ltd., Harlow, UK) source in LC chip coupling mode with an Orbitrap Fusion mass  
169 spectrometer (Thermo Fisher Scientific, Waltham, USA). Samples (5  $\mu$ L) were first loaded for  
170 5 min on the precolumn ( $\mu$ -pre-column, Acclaim PepMap C18, 2 cm, Thermo Scientific) at 4%  
171 mobile phase B (80% acetonitrile in nanopure water with 0.08% formic acid) and 96% mobile  
172 phase A (nanopure water with 0.1% formic acid) at a flow rate of 300 nl/min and at 35°C.  
173 Then they were eluted from the analytical column (Acclaim PepMap C18 LC column, 25 cm,  
174 Thermo Scientific) over a 100-min linear gradient of mobile phase B (4%–50%). The MS was  
175 set on Top Speed for 3 s using the Orbitrap analyzer for MS and MS/MS scans with higher  
176 energy collision dissoziation (HCD) fragmentation at normalized collision energy of 30%. MS  
177 scans were measured at a resolution of 120,000 in the scan range of 400–1,600  $m/z$ . The MS  
178 ion count target was set to  $4 \times 10^5$  at an injection time of 60 ms. Most intense peaks (charge  
179 state 2-7) were isolated for MS/MS scans by a quadrupole with an isolation window of 2 Da  
180 and were measured with a resolution of 15,000. The dynamic exclusion was set to 30 s with a  
181 +/-10 ppm tolerance. The automatic gain control target was set to  $5 \times 10^4$  with an injection time  
182 of 150 ms

## 183 **Bioinformatical analysis**

### 184 *Protein identification and quantification*

185 Proteome Discoverer (v2.1, Thermo Fischer Scientific) was used for protein identification and  
186 quantification (detailed workflow in Supplemental Methods). The MS/MS spectra (.raw files)  
187 were searched by Sequest HT against a database containing 3,233 non-redundant protein-  
188 coding sequence entries (downloaded January 2017 from NCBI GenBank, accession number  
189 CP007201.1). A “common repository of adventitious proteins database” (cRAP) was  
190 integrated to exclude contaminants. Trypsin was selected as protease and up to 2 missed  
191 cleavages, 10 ppm precursor and 0.02 Da fragment mass tolerance were allowed. Peptides  
192 with < 1% false discovery rate (FDR), XCorr  $\geq 2$ , q-value and the posterior error probability  
193 (PEP)  $\leq 0.01$  were considered as identified. Proteins were quantified using the average of top  
194 three peptide MS1-areas, yielding raw protein abundances. The mass spectrometry  
195 proteomics data (including the \*.raw- and result-files) have been deposited to the  
196 ProteomeXchange Consortium via the PRIDE (<https://www.ebi.ac.uk/pride>) partner repository  
197 with the dataset identifier PXD009308.

### 198 *Melting curve fitting, melting point determination, and significance test*

199 Raw protein abundances of all quantified proteins were log transformed and scaled between  
200 0 and 1 by subtracting the global minimum and normalizing to the abundance at the lowest  
201 temperature of each protein to yield fold changes (Fig. S3). Proteins with at least two  
202 abundance values in three replicates were considered as quantified. The average of these  
203 two or, if available, all three replicates was calculated for each temperature point and  
204 condition (criterion i). Furthermore, only proteins with an average quantitative value in at least  
205 five temperature points (ii) were considered for the melting curve analysis by the adapted *R*  
206 script TPP-TR [25, 26]. The melting curves were calculated using a sigmoidal fitting approach

207 with the *R* package *TPP*. This fitting was used to determine the melting point ( $T_m$ ), which is  
208 defined as the temperature at which half of the amount of proteins was denatured. The  
209 melting point differences ( $\Delta T_m$ ) were calculated by subtracting the  $T_m$  with ethanol from the  $T_m$   
210 with TCE [25, 26]. The sigmoidal melting curves were quality-filtered according to the  
211 following criteria [25, 26]: (iii) melting curves must reach a relative abundance plateau  $< 0.3$   
212 and (iv) the quality of the fit as expressed by the coefficient of determination ( $R^2$ ) of both, the  
213 TCE treated and control melting curves, must be  $> 0.8$  in at least two of three replicates. The  
214 statistical significance was calculated by using the non-parametric analysis of response  
215 curves (NPARC) of the *R* package *TPP*, comparing the spline progression of the TCE-treated  
216 condition and the ethanol-control [27]. The significance threshold was set to  $p < 0.01$ . This  
217 estimation was further adjusted by the Benjamini-Hochberg correction to exclude potential  
218 false positives [25, 26]. The quality-filtered melting curve data were used for figure generation  
219 in *R* v3.4.2, by using the *R* packages *graphics*, *stats*, and *heatmap*.

## 220 **Results**

221 We analyzed the melting proteome of *S. multivorans* in order to identify protein-substrate  
222 interactions of the reductive dehalogenase PceA with the substrate TCE. First, we modified  
223 the protocol [25] for analyzing oxygen-sensitive enzymes of bacteria. Therefore, cultivation of  
224 bacteria, cell harvesting, protein extraction, substrate treatment, and temperature incubation  
225 were performed under strictly anoxic conditions. A reductive dechlorination activity test of the  
226 crude extract revealed an initial specific enzyme activity of  $7.7 \pm 0.9$  nkat/mg with TCE as  
227 substrate, which decreased to  $2.8 \pm 0.5$  nkat/mg after cell lysis. This shows that the reductive  
228 dehalogenase did retain enzyme activity after sample preparation.

229 The samples were treated with either TCE or ethanol for the negative control. Afterward, the  
230 samples (each aliquot) were exposed to one out of ten different temperatures in the range of  
231  $43^\circ\text{C}$  to  $97^\circ\text{C}$ . The denatured proteins were separated from the native proteins by

232 ultracentrifugation. After mass spectrometric analysis of the native fraction and statistical  
233 analysis, the proteins were quality-filtered and fitted to protein melting curves. In total, 1,335  
234 of the identified proteins were quantified, which comprises about 42% of the predicted  
235 protein-coding sequences (Fig. 1).

236 In general, the protein abundances show that the native protein fractions decrease with  
237 increasing temperatures (Fig. 2A). This allowed the calculation of protein melting curves by  
238 sigmoidal curve fitting (Fig. 2B). After a stringent filtering procedure (Fig. S3), we obtained  
239 highly valid sigmoidal melting curves of 435 proteins (Fig. 1, Tab. S1), with an average  
240 standard error of 7%. Of all protein melting curves, 73% reached a plateau of zero at higher  
241 temperatures (e.g., Fig. 2B). Of the organohalide respiratory core region [13], 31 gene  
242 products were identified; for nine of them an average sigmoidal melting curve could be  
243 calculated and a melting curve analysis could be conducted (Fig. S1). Melting curves for  
244 proteins produced from the organohalide respiratory core region include the reductive  
245 dehalogenase PceA (SMUL\_1531, Fig. 3A), an IscU/NifU-like protein (SMUL\_1533) which  
246 might aid in PceA maturation, several proteins predicted to be involved in corrinoid synthesis  
247 (SMUL\_1544, 1545, 1547, 1548, 1551, 1559, 1560, 1562) and two flavin-containing proteins,  
248 the FeS-cluster binding flavoprotein (SMUL\_1573) and a putative flavin mononucleotide-  
249 binding protein (SMUL\_1575).

250 Melting temperatures ( $T_m$ ) were defined as the temperature at which half of the protein  
251 amount has been denatured (Tab. S1). The median  $T_m$  of all *S. multivorans* proteins was at  
252 73°C (Fig. S2). In order to assess the reproducibility of the TPP, the melting temperatures of  
253 the individual replicates were correlated to each other (Fig. 2C). The  $T_m$  values of two  
254 replicates each were linear fitted, yielding coefficients of determination ranging from  $R^2 = 0.58$   
255 to 0.84.

256 To show the effect of TCE treatment on the stability of the proteome, the  $T_m$  shift ( $\Delta T_m =$   
257  $T_{mTCE} - T_{mcontrol}$ ) and their adjusted p-values after Benjamini-Hochberg correction are

258 displayed (Fig. 2D). 82 proteins (19%) have a mean  $\Delta T_m$  outside the mean  $\pm 1$  standard  
259 deviation ( $\Delta T_m < -1.8^\circ\text{C}$  or  $\Delta T_m > 4.1^\circ\text{C}$ ). Of the 435 protein melting curves, 20 were  
260 significantly shifted, i.e., exhibit an adjusted  $p < 0.01$  (Tab. 1). These are candidates for an  
261 interaction with TCE. In total, five of the 20 significant protein melting curves fall outside both,  
262 the  $\Delta T_m$  and the significance threshold (Fig. 2D), including the reductive dehalogenase PceA  
263 ( $\Delta T_m = 5.5^\circ\text{C}$ , adj.  $p$ -value = 0.0028, Fig. 3A). The melting curve shift of the reductive  
264 dehalogenase was validated by western blot analysis (Fig. S4). In addition, the putative  
265 response regulator SMUL\_1539, most probably involved in the induction of PCE respiration,  
266 showed a  $\Delta T_m$  of  $4.6^\circ\text{C}$ , thus being outside the mean  $\Delta T_m \pm 1$  standard deviation threshold.  
267 This, however, could not be statistically tested (Fig. 3A), because of too many missing values  
268 in the curves (Tab. S1). The corresponding membrane-bound putative histidine kinase  
269 (SMUL\_1538) was not detectable.

270 Most proteins did not exhibit a significant melting curve shift (Fig. 2D). As representative  
271 examples, the melting curves of three proteins of different functional classes, localizations,  
272 and abundances (30-/40-/38-fold less abundant than PceA) are displayed (Fig. 3B). The  
273 tryptophan synthase (SMUL\_0559) is involved in the amino acid synthesis, the TetR family  
274 protein (SMUL\_1358) is a generic transcriptional regulator and the ATP synthase delta  
275 subunit (SMUL\_0684) is a membrane-associated representative of the energy metabolism.

## 276 **Discussion**

277 Direct detection of protein interactions in organohalide-respiring bacteria is a major challenge.  
278 Therefore, we modified the TPP method to monitor changes in protein thermal stability across  
279 the whole proteome of oxygen-sensitive bacterial cells and the substrate specificities of  
280 reductive dehalogenases. In total, about 33% of the quantified proteins yielded two high-  
281 quality average melting curves of at least two replicates each. Compared to Savitski *et al.*  
282 [19], we have fewer identifications, which is due to our label-free approach. However, our

283 results are similar to other label-free studies [28] and highly valid and reproducible due to our  
284 comprehensive statistical filtering procedure.

### 285 **Proof of enzyme-substrate interactions**

286 While the melting temperature of most background proteins was essentially unchanged by  
287 exposure to TCE, the reductive dehalogenase PceA exceeded the stringent p-value and  
288 melting temperature shift thresholds. The significant melting curve shift by TCE could be  
289 confirmed by western blot analysis. In former studies, PceA was shown to be able to  
290 dechlorinate TCE [10, 11]. The substrate specificity of PceA towards TCE was supported by  
291 TPP, providing a proof-of-concept that TPP is a suitable instrument to study enzyme-  
292 substrate interactions. The stabilization of an enzyme by its substrate first might sound  
293 counterintuitive, since a substrate, unlike a ligand, is converted by the enzyme. However, our  
294 data indicate that the enzyme-substrate complex endures long enough to induce a detectable  
295 stability shift of the enzyme. We promoted the stability of the enzyme-substrate complex by  
296 omitting the electron donor for the dehalogenating reaction, e.g., reduced methyl viologen,  
297 thereby blocking the transformation of TCE. Furthermore, we provided TCE in excess to be  
298 able to detect a PceA melting curve shift despite other electron donors in the cell lysate, e.g.,  
299 reduced ferredoxin, which also might reduce TCE. The binding of TCE to PceA was shown to  
300 occur mainly via van der Waals contacts in a hydrophobic active site pocket [30]. It is  
301 therefore comparable to the binding of, e.g., the inhibitor methotrexate to the dihydrofolate  
302 reductase, which occurs via intermolecular forces or, more specifically, ionic bonds [29] and  
303 was detectable by TPP [21].

304 A protein with a melting curve shift above the  $\Delta T_m$  threshold, which, however, did not pass the  
305 applied stringent filter criteria and therefore could not be tested for significance, was a  
306 putative response regulator (SMUL\_1539). SMUL\_1539 is part of the two-component system

307 presumably involved in regulating organohalide respiration [13]. According to the classical  
308 two-component regulatory system model [14], the histidine kinase would be the protein  
309 sensing the TCE and upon binding activating the response regulator by phosphorylation.  
310 Hence, the stabilization of the response regulator by TCE should be indirect. Thermal stability  
311 of a protein depends on bound ligands, posttranslational modifications, other proteins or  
312 cofactors. Savitski *et al.* [19] demonstrated how down-stream effectors exhibit  $T_m$  shifts, even  
313 if the effectors do not bind the ligand themselves: Kinase inhibitor treatment did not only  
314 cause  $T_m$  shifts of kinases but also of a phosphatase and an adaptor protein binding  
315 phosphorylated proteins. To date, the role of the two-component system in *S. multivorans* has  
316 only been inferred from the localization of the respective genes in the genome, sequence  
317 alignments and proteomic studies [12, 13]. More detailed biochemical analyses failed  
318 because of the difficulties when working with organohalide-respiring bacteria, including the  
319 unfeasible genetic manipulation and obstructed heterologous expression. Therefore, our data  
320 on the indirect interaction of the putative response regulator SMUL\_1539 with TCE offer a  
321 valuable indication about the transmission of the signal from trichloroethene to expression of  
322 the organohalide respiratory gene region gene region.

323 The unaltered melting curves of most proteins support the hypothesis that only a few proteins  
324 directly interact with TCE, corresponding to the observation that most of the genes outside  
325 the organohalide respiratory region have orthologs also in non-dehalogenating  
326 *Sulfurospirillum* spp. [12].

### 327 **Other proteins affected by TCE**

328 Besides PceA, 19 further proteins with significant TCE-induced thermal stability changes  
329 were identified. Those neither have any hypothesized relation to organohalide respiration nor  
330 are encoded in any cluster supposed to be involved in organohalide respiration [12] nor were

331 specifically induced by chlorinated ethenes [13]. Therefore, we assume that these proteins  
332 bind TCE unspecifically and do not have any physiological role in organohalide respiration of  
333 *S. multivorans*. This can be promoted by the molecular size of the substrates of some of  
334 these proteins, i.e., fumarate and pyruvate (fumarate reductase iron-sulfur protein,  
335 SMUL\_552; acetolactate synthase small subunit, SMUL\_1644). In general, biophysical  
336 methods such as ligand-binding studies using thermal shift assays on purified proteins are  
337 considered to produce only a few false-positive results [21]. Our study is in line with that,  
338 yielding 4.4% unspecific background binders.

### 339 **Protocol adaptations to TCE-tolerant, oxygen-sensitive bacteria**

340 Peng *et al.* [31] used *E. coli* protein extract and quantified the denatured protein fraction.  
341 They observed that at their highest chosen temperature, 70°C, most proteins are still in  
342 solution. We circumvented this challenge by increasing the maximum temperature from  
343 approximately 70°C, which was also as the highest temperature used in most other studies  
344 on mammalian cells [19, 32, 33], to 97°C. Thus, in our study, the melting curves of the  
345 majority of proteins reached a base of zero at the highest temperatures. The median melting  
346 point of the *S. multivorans* proteins (73°C) lies between the  $T_m$ -median of human cells, yeast  
347 or *E. coli* (51-59°C) and *Thermus thermophilus* (81°C) [19, 26, 28]. Since *S. multivorans* is a  
348 mesophilic organism, the elevated median melting point might hint at an adaptation of the  
349 proteins towards solvent stress, to which proteins might develop similar strategies as towards  
350 heat, such as inflexibility, compactness and core hydrophobicity [34]. However, further TPP  
351 studies with other bacteria are required to prove the reason for the specific protein melting  
352 points.

353 Important to note is that we modified our protocol in order to exclude oxygen during cell  
354 harvesting, protein extraction, substrate, and temperature incubation. All working steps were

355 accomplished in an anoxic chamber or in gas-tight tubes and by adding cysteine to all used  
356 buffers. These modifications were preceded by an elaborate optimization procedure. Another  
357 challenge of using TPP for bacterial applications is that protein extraction is not as efficient  
358 and reproducible as in mammalian cells [35]. As a consequence, instead of using intact cells  
359 for substrate and temperature incubation, we used aliquoted cell lysate.

### 360 **Future implications**

361 The benefit of TPP is that protein-protein and protein-substrate interactions can be  
362 investigated under nearly physiological conditions. TPP is therefore highly suitable for  
363 organohalide-respiring bacteria because related studies suffer from high oxygen sensitivity of  
364 their enzymes, poor biomass yields, impeded enzyme purification and missing heterologous  
365 expression systems. As we have shown in our study, TPP is a favorable screening method to  
366 reduce the list of potential proteins interacting with halogenated compounds for subsequent  
367 molecular biochemical validations.

368 In the future, TPP could resolve substrate specificities of reductive dehalogenases with  
369 unresolved substrate spectrum, e.g., of *Dehalococcoides mccartyi*, *Dehalobacter restrictus* or  
370 *Desulfitobacterium spp.*, which harbor several reductive dehalogenases [15, 36-38]. It might  
371 also serve to elucidate the association of reductive dehalogenases with the respiration  
372 complex by comparing the  $T_m$  values of different reductive dehalogenases. In *D. mccartyi*,  
373 several studies indicate that electron transfer does not occur via a classical electron transport  
374 chain involving quinones but within a large multiprotein complex, the composition of which is  
375 not completely resolved [17, 18]. The suitability of TPP for studying protein complexes was  
376 demonstrated by Savitski *et al.* [19] and Bai *et al.* [39].

### 377 **Conclusion**

378 The protein interaction of a reductive dehalogenase with its specific substrate was  
379 demonstrated using the TPP method. Additionally, we found indications that the response  
380 regulator, at least indirectly, interacts with TCE. Our findings provide useful complementary  
381 information on their protein stability. The TPP protocol is transferable to other bacteria, even  
382 though the optimal temperature range needs to be defined for the organism and proteins of  
383 interest. To test the protein binding to one substrate, approximately 3 mg protein amount is  
384 required per replicate, with additional 1.5 mg per additional substrate. TPP will further help us  
385 to resolve the specificities and regulatory circuits of reductive dehalogenases towards many  
386 different substrates, which are among the most unresolved fields in research on  
387 organohalide-respiring bacteria, but also to gain insights into the physiology of other slow-  
388 growing or difficult to study bacteria.

## 389 **Acknowledgment**

390 This work was supported by the German Research Foundation (DFG), as part of the research  
391 group FOR 1530. D.T. was also supported by the Helmholtz Interdisciplinary Graduate  
392 School for Environmental Research (HIGRADE). The authors are grateful for the use of the  
393 analytical facilities of the Centre for Chemical Microscopy (ProVIS) at the Helmholtz Centre  
394 for Environmental Research, which is supported by European Regional Development Funds  
395 (EFRE - Europe funds Saxony) and the Helmholtz Association. Benjamin Scheer is thankfully  
396 acknowledged for maintenance of the Orbitrap Fusion mass spectrometer.

## 397 **References**

- 398 [1] ATSDR, Agency for toxic substances and disease registry's Substance Priority List, 2017.  
399 [2] IPCS, International Programme for Chemical Safety, Environmental health criteria 195, 1997.  
400 [3] IPCS, International Programme for Chemical Safety, Environmental health criteria 140, 1993.  
401 [4] IPCS, International Programme for Chemical Safety, Environmental health criteria 71, 1987.  
402 [5] J. Koenig, M. Lee, M. Manefield, Aliphatic organochlorine degradation in subsurface environments,  
403 Rev. Environ. Sci. Biotechnol. 14(1) (2015) 49-71.

404 [6] D. Leys, L. Adrian, H. Smidt, Organohalide respiration: microbes breathing chlorinated molecules,  
405 Philos. Trans. R. Soc. Lond., Ser. B: Biol. Sci. 368(1616) (2013).

406 [7] S. Atashgahi, Y. Lu, H. Smidt, Overview of Known Organohalide-Respiring Bacteria—Phylogenetic  
407 Diversity and Environmental Distribution, in: L. Adrian, F.E. Löffler (Eds.), Organohalide-Respiring  
408 Bacteria, Springer Berlin Heidelberg, Berlin, Heidelberg, 2016, pp. 63-105.

409 [8] H. Dobbek, D. Leys, Insights into Reductive Dehalogenase Function Obtained from Crystal  
410 Structures, in: L. Adrian, F.E. Löffler (Eds.), Organohalide-Respiring Bacteria, Springer Berlin  
411 Heidelberg, Berlin, Heidelberg, 2016, pp. 485-495.

412 [9] T. Schubert, L. Adrian, R.G. Sawers, G. Diekert, Organohalide respiratory chains: composition,  
413 topology and key enzymes, FEMS Microbiol. Ecol. 94(4) (2018) fiy035.

414 [10] A. Neumann, G. Wohlfarth, G. Diekert, Purification and Characterization of Tetrachloroethene  
415 Reductive Dehalogenase from *Dehalospirillum multivorans*, J. Biol. Chem. 271(28) (1996) 16515-  
416 16519.

417 [11] C. Kunze, M. Bommer, W.R. Hagen, M. Uksa, H. Dobbek, T. Schubert, G. Diekert, Cobamide-  
418 mediated enzymatic reductive dehalogenation via long-range electron transfer, Nat. Commun. 8  
419 (2017) 15858.

420 [12] T. Goris, T. Schubert, J. Gadkari, T. Wubet, M. Tarkka, F. Buscot, L. Adrian, G. Diekert, Insights into  
421 organohalide respiration and the versatile catabolism of *Sulfurospirillum multivorans* gained from  
422 comparative genomics and physiological studies, Environ. Microbiol. 16(11) (2014) 3562-3580.

423 [13] T. Goris, C.L. Schiffmann, J. Gadkari, T. Schubert, J. Seifert, N. Jehmlich, M. von Bergen, G.  
424 Diekert, Proteomics of the organohalide-respiring Epsilonproteobacterium *Sulfurospirillum*  
425 *multivorans* adapted to tetrachloroethene and other energy substrates, Sci. Rep. 5 (2015) 13794.

426 [14] E.A. Groisman, Feedback Control of Two-Component Regulatory Systems, Annu. Rev. Microbiol.  
427 70(1) (2016) 103-124.

428 [15] D. Türkowsky, N. Jehmlich, G. Diekert, L. Adrian, M.v. Bergen, T. Goris, An integrative overview of  
429 genomic, transcriptomic and proteomic analyses in organohalide respiration research, FEMS  
430 Microbiol. Ecol. 94(3) (2018) fiy013.

431 [16] L. Adrian, J. Rahnenführer, J. Gobom, T. Hölscher, Identification of a Chlorobenzene Reductive  
432 Dehalogenase in *Dehalococcoides* sp. Strain CBDB1, Appl. Environ. Microbiol. 73(23) (2007) 7717-  
433 7724.

434 [17] A. Kublik, D. Deobald, S. Hartwig, C.L. Schiffmann, A. Andrades, M. von Bergen, R.G. Sawers, L.  
435 Adrian, Identification of a multi-protein reductive dehalogenase complex in *Dehalococcoides mccartyi*  
436 strain CBDB1 suggests a protein-dependent respiratory electron transport chain obviating quinone  
437 involvement, Environ. Microbiol. 18(9) (2016) 3044-3056.

438 [18] S. Hartwig, N. Dragomirova, A. Kublik, D. Türkowsky, M. von Bergen, U. Lechner, L. Adrian, R.G.  
439 Sawers, A H<sub>2</sub>-oxidizing, 1,2,3-trichlorobenzene-reducing multienzyme complex isolated from the  
440 obligately organohalide-respiring bacterium *Dehalococcoides mccartyi* strain CBDB1, Environ.  
441 Microbiol. Rep. 9(5) (2017) 618-625.

442 [19] M.M. Savitski, F.B. Reinhard, H. Franken, T. Werner, M.F. Savitski, D. Eberhard, D. Martinez  
443 Molina, R. Jafari, R.B. Dovega, S. Klaeger, B. Kuster, P. Nordlund, M. Bantscheff, G. Drewes, Tracking  
444 cancer drugs in living cells by thermal profiling of the proteome, Science 346(6205) (2014) 1255784.

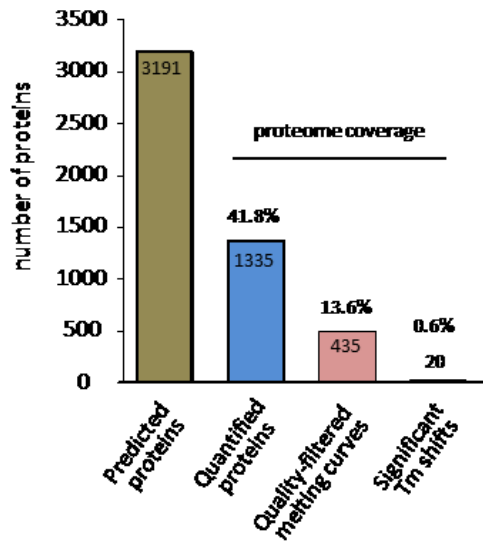
445 [20] A. Mateus, T.A. Määttä, M.M. Savitski, Thermal proteome profiling: unbiased assessment of  
446 protein state through heat-induced stability changes, Proteome Science 15 (2016) 13.

447 [21] D. Martinez Molina, R. Jafari, M. Ignatushchenko, T. Seki, E.A. Larsson, C. Dan, L. Sreekumar, Y.  
448 Cao, P. Nordlund, Monitoring Drug Target Engagement in Cells and Tissues Using the Cellular Thermal  
449 Shift Assay, Science 341(6141) (2013) 84-87.

450 [22] J. Gadkari, T. Goris, C.L. Schiffmann, R. Rubick, L. Adrian, T. Schubert, G. Diekert, Reductive  
451 tetrachloroethene dehalogenation in the presence of oxygen by *Sulfurospirillum multivorans*:  
452 physiological studies and proteome analysis, *FEMS Microbiol. Ecol.* 94(1) (2018) fix176-fix176.  
453 [23] H. Scholz-Muramatsu, A. Neumann, M. Meßmer, E. Moore, G. Diekert, Isolation and  
454 characterization of *Dehalospirillum multivorans* gen. nov., sp. nov., a tetrachloroethene-utilizing,  
455 strictly anaerobic bacterium, *Arch. Microbiol.* 163(1) (1995) 48-56.  
456 [24] M. John, R. Rubick, R.P. Schmitz, J. Rakoczy, T. Schubert, G. Diekert, Retentive memory of  
457 bacteria: Long-term regulation of dehalorespiration in *Sulfurospirillum multivorans*, *J. Bacteriol.*  
458 191(5) (2009) 1650-1655.  
459 [25] H. Franken, T. Mathieson, D. Childs, G.M.A. Sweetman, T. Werner, I. Tögel, C. Doce, S. Gade, M.  
460 Bantscheff, G. Drewes, F.B.M. Reinhard, W. Huber, M.M. Savitski, Thermal proteome profiling for  
461 unbiased identification of direct and indirect drug targets using multiplexed quantitative mass  
462 spectrometry, *Nat. Protoc.* 10 (2015) 1567.  
463 [26] F.B.M. Reinhard, D. Eberhard, T. Werner, H. Franken, D. Childs, C. Doce, M.F. Savitski, W. Huber,  
464 M. Bantscheff, M.M. Savitski, G. Drewes, Thermal proteome profiling monitors ligand interactions  
465 with cellular membrane proteins, *Nat. Methods* 12 (2015) 1129.  
466 [27] D. Childs, N. Kurzawa, Introduction to the TPP package for analyzing Thermal Proteome Profiling  
467 data: Temperature range (TR) or concentration compound range (CCR) experiments (2016).  
468 [28] P. Leuenberger, S. Gansch, A. Kahraman, V. Cappelletti, P.J. Boersema, C. von Mering, M.  
469 Claassen, P. Picotti, Cell-wide analysis of protein thermal unfolding reveals determinants of  
470 thermostability, *Science* 355(6327) (2017).  
471 [29] H.B. Schlegel, M. Poe, K. Hoogsteen, Models for the Binding of Methotrexate to *Escherichia coli*  
472 Dihydrofolate Reductase, *Mol. Pharmacol.* 20(1) (1981) 154.  
473 [30] M. Bommer, C. Kunze, J. Fessler, T. Schubert, G. Diekert, H. Dobbek, Structural basis for  
474 organohalide respiration, *Science* 346(6208) (2014) 455-458.  
475 [31] H. Peng, H. Guo, O. Pogoutse, C. Wan, L.Z. Hu, Z. Ni, A. Emili, An Unbiased Chemical Proteomics  
476 Method Identifies FabI as the Primary Target of 6-OH-BDE-47, *Environ. Sci. Technol.* 50(20) (2016)  
477 11329-11336.  
478 [32] B.X. Tan, C.J. Brown, F.J. Ferrer, T.Y. Yuen, S.T. Quah, B.H. Chan, A.E. Jansson, H.L. Teo, P.  
479 Nordlund, D.P. Lane, Assessing the Efficacy of Mdm2/Mdm4-Inhibiting Stapled Peptides Using Cellular  
480 Thermal Shift Assays, *Sci. Rep.* 5 (2015) 12116.  
481 [33] J.-J. Qin, W. Wang, S. Voruganti, H. Wang, W.-D. Zhang, R. Zhang, Identification of a new class of  
482 natural product MDM2 inhibitor: *In vitro* and *in vivo* anti-breast cancer activities and target validation,  
483 *Oncotarget* 6(5) (2015) 2623-2640.  
484 [34] Y. Ding, Y. Cai, Y. Han, B. Zhao, Comparison of the structural basis for thermal stability between  
485 archaeal and bacterial proteins, *Extremophiles* 16(1) (2012) 67-78.  
486 [35] S.C. Tan, B.C. Yiap, DNA, RNA, and Protein Extraction: The Past and The Present, *J. Biomed.*  
487 *Biotechnol.* 2009 (2009) 574398.  
488 [36] L.A. Hug, F. Maphosa, D. Leys, F.E. Löffler, H. Smidt, E.A. Edwards, L. Adrian, Overview of  
489 organohalide-respiring bacteria and a proposal for a classification system for reductive  
490 dehalogenases, *Philos. Trans. R. Soc. Lond., Ser. B: Biol. Sci.* 368(1616) (2013) 20120322.  
491 [37] T. Kruse, T. Goris, J. Maillard, T. Woyke, U. Lechner, W. de Vos, H. Smidt, Comparative genomics  
492 of the genus *Desulfitobacterium*, *FEMS Microbiol. Ecol.* 93(12) (2017) fix135.  
493 [38] T. Kruse, J. Maillard, L. Goodwin, T. Woyke, H. Teshima, D. Bruce, C. Detter, R. Tapia, C. Han, M.  
494 Huntemann, C.-L. Wei, J. Han, A. Chen, N. Kyrpides, E. Szeto, V. Markowitz, N. Ivanova, I. Pagani, A.  
495 Pati, S. Pitluck, M. Nolan, C. Holliger, H. Smidt, Complete genome sequence of *Dehalobacter restrictus*  
496 PER-K23<sup>T</sup>, *Stand. Genomic Sci.* 8(3) (2013) 375-388.

497 [39] L. Bai, J. Chen, D. McEachern, L. Liu, H. Zhou, A. Aguilar, S. Wang, BM-1197: A Novel and Specific  
498 Bcl-2/Bcl-xL Inhibitor Inducing Complete and Long-Lasting Tumor Regression *In Vivo*, PLoS One 9(6)  
499 (2014) e99404.

500 **Figures**

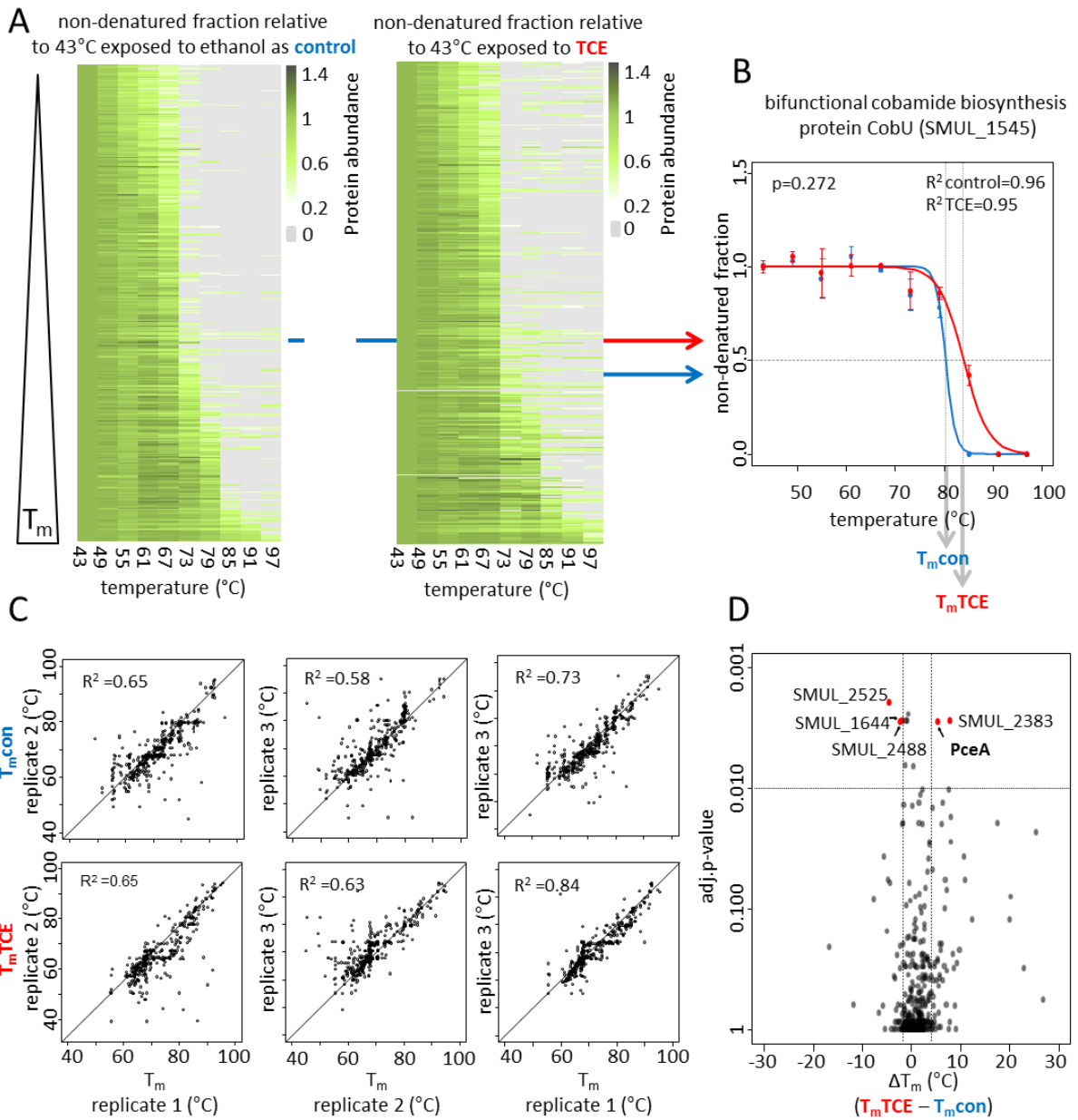


501

502 Fig. 1. Proteome coverage of *S. multivorans*. The predicted proteome is compared to the  
503 number of quantified proteins, sigmoidal protein melting curves, and protein melting curves  
504 with a significant shift.

505

506

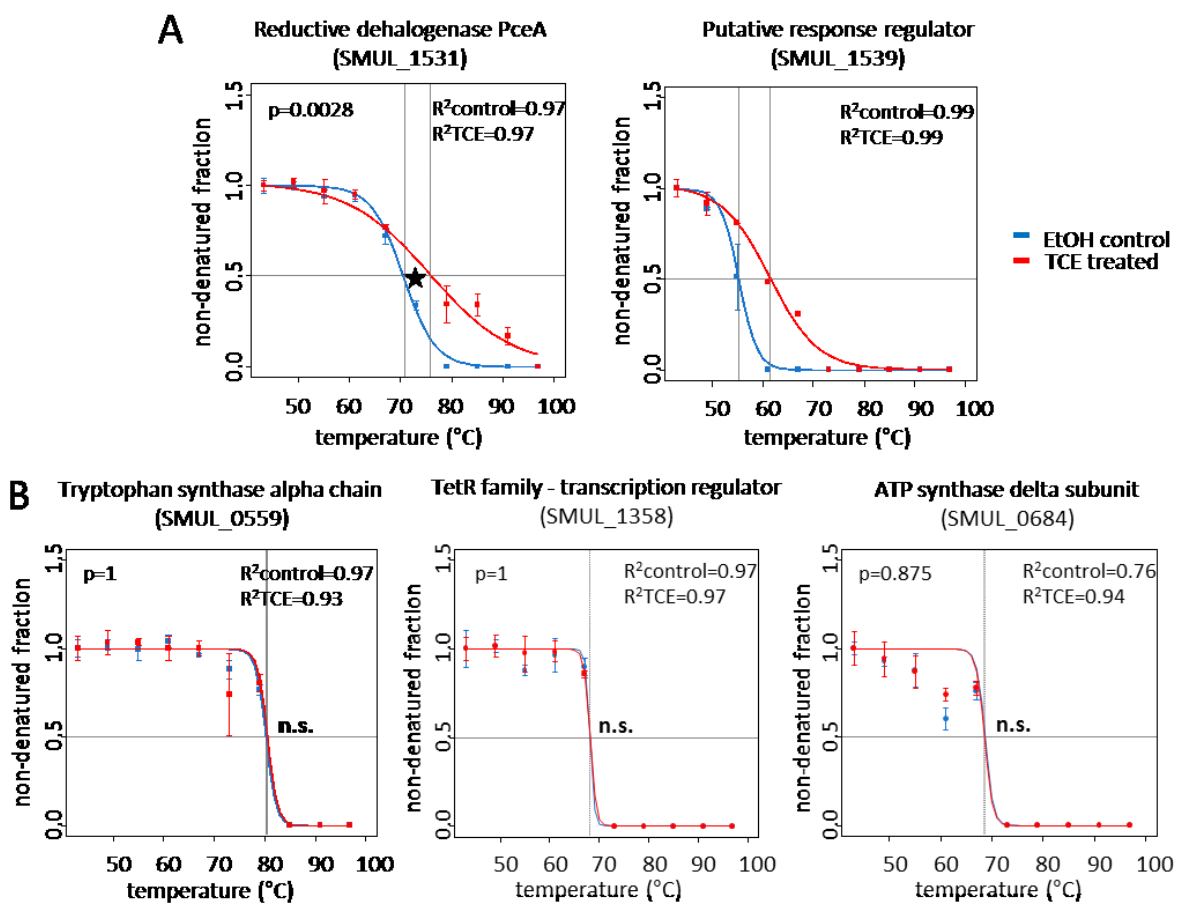


507

508 Fig. 2. (A) Heatmap of the thermal stability of all proteins exposed to trichloroethene (TCE,  
 509 right) or ethanol as a control (left). The colors indicate protein abundance levels of the non-  
 510 denatured protein fractions after incubation at one of ten temperatures. Shown are relative  
 511 abundances normalized to the abundance after incubation to the lowest temperature (43°C).  
 512 Each line represents the average of at least two replicates of a protein. (B) Two  
 513 representative protein melting curves with and without TCE treatment, calculated by a  
 514 sigmoidal fitting approach over the temperature range. The melting temperature ( $T_m$ )  
 515 represents the temperature at which half of the protein is denatured. (C) The reproducibility of

516 the thermal proteome profiling displayed by the coefficient of determination ( $R^2$ ) of the  $T_m$  of  
 517 two replicates each. (D) Volcano plot of the melting temperature differences ( $\Delta T_m$ ) between  
 518 TCE-exposed and control-proteins and their Benjamini-Hochberg adjusted p-values. The  
 519 vertical and horizontal lines mark the threshold for adjusted p-value ( $< 0.01$ ) and  $\Delta T_m$  (mean  $\pm$   
 520 1 standard deviation). SMUL\_2525, acetyl-coenzyme A; SMUL\_1644, acetolactate synthase  
 521  $\alpha$ -subunit; SMUL\_2488, phosphomannomutase/phosphoglucomutase; SMUL\_2383,  
 522 hydrogenase-4 component A; PceA, reductive dehalogenase.

523



524

525 Fig. 3. Protein-substrate interactions of selected proteins. (A) Melting curves of PceA and the  
 526 response regulator (both are encoded in the organohalide respiratory gene region) showed a  
 527 melting temperature ( $T_m$ ) shift towards higher temperatures upon trichloroethene (TCE)  
 528 treatment. (B) Three examples of protein melting curves with no significant  $T_m$  shifts after  
 529 TCE treatment. Y-axes give  $\log_2$  fold changes of the non-denatured proteins relative

530 to 43°C. Error bars indicate standard errors of n=3 at ten different temperature points. A  
 531 significant protein melting curve shift (adj. p < 0.01) is represented by an asterisk. R<sup>2</sup> =  
 532 coefficient of determination.

533

534 Table 1. Proteins with a significant melting curve shifts. The p-values are adjusted according  
 535 to Benjamini-Hochberg and the reductive dehalogenase PceA is highlighted in red.

Accession no.	Protein name	adj. p-value	ΔTm (°C)
SMUL_2383_2340	hydrogenase-4 component A, iron-sulfur cluster containing subunit	3E-06	12.0
SMUL_0693_673	outer membrane lipoprotein omp16-like	3E-03	7.8
SMUL_1531_1502	tetrachloroethene reductive dehalogenase catalytic subunit PceA	3E-03	5.5
SMUL_0481_468	LSU ribosomal protein L11p (L12e)	7E-04	2.5
SMUL_0593_579	peptide chain release factor 2	2E-05	1.3
SMUL_2819_2768	L-asparaginase	4E-05	1.0
SMUL_2009_1975	phosphoribosylaminoimidazole-succinocarboxamide synthase	7E-03	0.5
SMUL_0563_549	translation elongation factor Ts	2E-03	-0.6
SMUL_2097_2063	hypothetical protein	3E-03	-0.8
SMUL_2912_2859	YceI family protein	3E-03	-1.1
SMUL_0552_538	fumarate reductase iron-sulfur protein	7E-03	-1.2
SMUL_2488_2444	phosphomannomutase / phosphoglucomutase	3E-03	-1.8
SMUL_1644_1613	acetolactate synthase small subunit	8E-03	-2.2
SMUL_2525_2481	acetyl-coenzyme A carboxyl transferase alpha chain	2E-03	-4.5
SMUL_1909_1875	hypothetical protein	6E-03	-
SMUL_2989_2936	hypothetical protein	1E-03	-
SMUL_0850_828	uridylate kinase	3E-03	-
SMUL_0273_266	molybdopterin oxidoreductase, chain B	6E-03	-
SMUL_1442_1414	isocitrate dehydrogenase [NADP]	3E-03	-
SMUL_1098_1075	single-stranded DNA-binding protein	2E-05	-

536

537